Journal of Advanced Zoology

ISSN: 0253-7214
*Volume **44** Issue **S-6 Year 2023** Page **1690:1698***

Creationa and Assessment of Dry Powder Inhalation Formulations of Gamma Oryzanol Based on Chitosan Nanoparticles

Vivek Kumar Patel[1], Rajsekaran S[2]

[1,2]Bhagwant University, Ajmer, Rajasthan.
Email: vivekptl428@gmail.com

**Corresponding author's E-mail: vivekptl428@gmail.com*

Article History

Received: 08 June 2023
Revised: 21 Sept 2023
Accepted: 08 Dec 2023

CC License
CC-BY-NC-SA 4.0

Abstract

Gamma oryzanol is an antioxidant and anticancer medication that is taken orally by a traditional method. It comes from plants. Its utility is nonetheless restricted by its erratic absorption and frequent administration. An alternative method that can maintain the release of Gamma Oryzanol in the lungs for several hours was considered: giving the drug via the pulmonary route as nanoparticles. Gamma Oryzanol was coated with chitosan, a biodegradable polymer, and then freeze-dried to create a dry powder inhaler (DPI) with an aerodynamic particle size of 1.54µm. Initial burst release was seen in an in vitro release investigation, which was followed by continuous release up to 97.51% in 24 hours. In vivo research and in vitro release showed further correlation. After a single dosage was administered, the prepared DPI enhanced the Gamma Oryzanol via pulmonary route residence in the lung tissue for more than 24 hours and sustained the Gamma Oryzanol through pulmonary pathway concentration above MIC for more than 12 hours. A decrease in the amount administered in the lungs was also seen in an animal investigation; this will help with tumour treatment.

Keywords: *Creation , Assesment*

1. Introduction

At 2%, gamma-oryzanol makes up the majority of the rice bran extract. Rice bran oil is made up of a variety of phytosteryl ferulates. Numerous studies highlight the health benefits of rice bran oil, including its ability to lower plasma cholesterol, limit platelet aggregation, and have specific antioxidant properties. Rice bran oil has been used in traditional Japanese medicine to alleviate gastrointestinal issues, promote skin capillary circulation, stimulate development, and lessen the symptoms of menopause. Strong antioxidant activity has been linked to chemotherapy, cancer, and the radioprotective impact. Numerous scholarly publications have documented the potential of gamma-oryzanol and rice bran oil, owing to their antioxidant properties, in the management of dyslipidemia. Patients with type 2 diabetes who drink rice bran oil modified milk on a regular basis report considerably lower overall blood cholesterol amount and a tendency to down cholesterol linked to minimize density lipoprotein (Lai et al., 2012).

In human and animal mockups, gamma-oryzanol and rice bran oil reduce serum whole part of cholesterol by obstructive lipid absorption from the intestine; the mechanism explaining the anti-inflammatory effect is reticence of nuclear factor-kB start via the antioxidant activit. Strong anti-inflammatory and radical scavenger properties are exhibited by gamma-oryzanol rich extracts potentially due to the abundance of powerful antioxidants, these extracts also up-regulate genes associated with antioxidants and down-regulate oxidative stress gene markers. Gamma-oryzanol may use the antioxidant pathway to impede the carcinogenic process. Ghatak and Panchal examined the immunomodulatory impending of oryzanol derived from raw rice bran oil using experimental animal models. Researchers found that oryzanol has sufficient capacity to stimulate humoral and cellular immune responses. In tumor-bearing mice, gamma-oryzanol can reduce tumour bulk associated with pro-angiogenic markers. The study conducted by Kim et al. (2012) revealed a noteworthy decrease in the mRNA and protein expression of vascular endothelial growth factor, 5-lipoxygenase-5 and cyclooxygenase-2. This resulted in the downregulation of VEGF and neoangiogenic inhibition inside the tumours, which in turn led to a decrease in the number of blood vessels within the tumour mass.

These findings point to the potential use of gamma-oryzanol in cancer treatment. Nevertheless, there aren't many published studies demonstrating gamma-oryzanol's anticarcinogenic properties. Because of the high correlation between oxidative stress and prostate cancer that has been shown in earlier research, prostate cancer cell lines were used as a model for cancer therapy. One possible treatment approach for prostate cancer cells, including the cancer-initiating cells, migration, and invasion, is to modify their redox status. According to Tangjitjaroenkun et al. (2012), reducing excessive reactive oxygen species (ROS) may be a highly efficient way to stop the development and spread of prostate cancer. To make the initiative unique, an alternate strategy was considered that would vary the dose form (nanoparticles) and route (pulmonary) for successful tumour treatment. Gamma-oryzanol in nanoparticulate form is able to evade phagocytic macrophages and penetrate intracellular compartments. Gamma-oryzanol was previously coated with Polylactic Co-Glycolic Acid (PLGA) Resomer RG-755S. However, 73±77% D, L lactide and 23±27% glycolide are present in this PLGA grade. It took longer to degrade because there were fewer glycolide units [5]. As a consequence, as previously reported [6], 43.52% of the gamma-oryzanol was released from PLGA nanoparticles in a 24-hour period. Therefore, there was a possibility of dosage dumping in the daily consumption. An alternative biodegradable polymer that could emit 90±100% gamma-oryzanol in 24 hours was required to solve this issue. Because of its low immunogenicity, cheap cost, and biocompatibility, chitosan—a partly deacetylated counterpart of chitin made of N-acetylglucosamine—has become an important biomaterial and pharma excipient for drug administration [7]. In the fields of medicine and pharmaceuticals, chitosan is widely used. It is utilised as a disintegrant, film coating substance, tablet excipient, to enhance medication disintegration, and to regulate drug release [8].

Moreover, it has been used to gel, films, beads, microspheres/microparticles, capsules, and nanoparticles [9]. Chitosan has been effectively used in the delivery of many organs, including the liver, kidney, lung, and others [10]. Additionally, it can facilitate macromolecule penetration through neatly arranged epithelia and is mucoadhesive [11]. It has been demonstrated that this polycationic polymer may interact with electrically negative materials to produce a core shell nanostructure, which shows great promise as a drug carrier [12]. Gamma-oryzanol nanoparticles coated with chitosan offer better drug loading, longer-lasting release, improved drug stability, and precisely targeted deposition [13].

2. Materials And Methods

We bought Gamma Oryzanol from YarrowChem in Mumbai, India. Himedia and Sigma Aldrich provided chitosan (>75% deacetylation) and sodium tripolyphosphate (TPP), respectively. A gift sample of inhalable grade lactose anhydrous (INH 40M 55.115) was acquired from the Kerry group in the United States. Analytical grade chemicals from Merck Millipore, Mumbai, India, were utilised for all other compounds. We received a gift sample of a nasal insufflator and a mono-dose inhaler from Milano, Italy.

Drug Excipient Interaction Study

Utilising Perkin Elmer (Massachusetts, USA), FTIR evaluation was conducted to examine the chemical relationship between Gamma Oryzanol, inhalable aqueous Lactose, and Chitosan. Two samples were analysed independently for pure Gamma Oryzanol and a physical combination of Gamma-oryzanol, and Chitosan, inhalable anhydrous Lactose,. The specimens were scanned in the infrared spectrum, 400–4000 cm−1.

Formultion of Gamma-Oryzanol Nanoparticles

Ionic gelation, with slight modifications, was used to create chitosan/TPP nanoparticles as previously described [13–14]. In short, at room temperature, chitosan (5 mg/ml) was submerged in a watery solution of acetic acid while being stirred magnetically. With frequent stirring, gamma oryzanol was distributed throughout the aforementioned chitosan solution. With constant stirring, TPP aqueous solution has been added drop by drop with a syringe needle to the gamma-oryzanol-containing chitosan solution mentioned above. For the predetermined amount of time, the stirring was continued. After a 30-minute centrifugation at 31150g (relative centrifugal force), the resulting nano-suspension was once again washed with distilled water. Since centrifugation generates excessive heat, a temperature of -4C was maintained throughout to stabilise the nanoparticles. The produced suspension should be freeze-dried with 2% w/v mannitol used as a cryprotectant. In this procedure, -20¯C was used for initial drying and -60ïC for secondary drying. To produce acceptable nanoparticles for the preparation of a dry powder inhaler, a number of process parameters, including stirring duration, the ratios of chitosan to TPP and gamma oryzanol, and the quantities of TPP solution, were optimised.

Characterization

The determination of the % drug entrapment (PDE) of (GO) in nanoparticles was achieved using ultracentrifugation at 31150g for 30 minutes, after the nanoparticles were separated from the aqueous medium. Using a UV spectrophotometer set at 288 nm, the quantity of free Gamma Oryzanol in the supernatant was determined [15]. Additional assessment metrics were computed in accordance with earlier reports [16]. The stability of the nanoparticles in the suspension was assessed by measuring the zeta potential, which represents the surface charge on the particles [17]. The particle size distribution of nanoparticles in a particular sample is shown by the gamma Oryzanol value. A higher PDI value denotes the distribution of variable-sized nanoparticles, which can lead to the development of aggregates, low homogeneity, and low stability of particle suspension.

As previously indicated, Zetasizer (Malvern, UK) was used to estimate the zeta size, zeta potential, (PDI) [17]. Choosing the TPP solution, acetic acid strength, and acid volume. In acidic environments, chitosan totally dissolves. A variation in the proportion of acetic acid solution [19, 20] was documented in the chitosan nanoparticle formulation. Since chitosan and gamma ryzanol both soluble in acetic acid, 1% v/v was chosen as the proportion. The initial volumes of the TPP solution and acetic acid were chosen to be 5 mL and 10 mL, respectively [21].

Effect of stirring time: In order to produce homogenous Gamma Oryzanol nanoparticles, stirring time is crucial. Thus, stirring time was adjusted while maintaining the same values for the other process parameters, such as the 6:1 chitosan-to-TPP ratio, the 5 mL TPP solution volume, and the 50:50 chitosan-to-gamma oryzanol weight ratio. Four different stirring times—15, 30, 60, and 45 minutes—were used to examine the effects of stirring time on the mean particle size, zeta potential, and PDE [13, 14, 22, 23, 24, 24]. Optimised formulation was selected based on increased PDE and smaller particle size. Chitosan and TPP ratio's effects. For the Chitosan-TPP ratio, gamma oryzanol nanoparticles were further optimised. Other procedure variables were held constant during this optimisation. Four novel ratios, such as 5:1, 4:1, 3:1, and 2:1, were chosen from the literature [22–25]. These ratios were used to create nanoparticles, which were then compared to an optimised 6:1 ratio following a stirring period. The volumes of the TPP solution and acetic acid were kept at 10 mL and 5 mL, respectively. This ratio was used to produce nanoparticles, and its impact on the physiological properties of the particles was investigated.

Effect of Gamma Oryzanol: ratio of chitosan. The gamma-oryzanol:chitosan ratio was optimised while maintaining the same values for all other process parameters. By varying the concentration of chitosan (60, 70, 80, and 90 mg) in relation to a set amount of gamma oryzanol, four distinct formulations were created. Additionally, the impact of chitosan quantity on PDE and particle size was examined. Since the 1% acetic acid volume was limited to 10 millilitres, a maximum of 90 milligrammes of chitosan could be added. Therefore, in order to compare with 1:1 (GT2), the Gamma Oryzanol -Chitosan ratios of 1:1.2, 1:1.4, 1:1.6, and 1:1.8 were created. Volume of TPP solution's effect. In order to see how the TPP solution affected the physicochemical characteristics of gamma-oryzanol nanoparticles, the volume of TPP solution was raised from 5 mL to 10 mL (while maintaining the same TPP quantity).

SEM, or scanning electron microscopy. The Gamma Oryzanol nanoparticles' form and surface morphology were investigated using Karl Zesis scanning electron microscopy (VO-18, SE detector). The samples underwent gold sputter coating, and they were examined for morphology at a voltage of 6.0 kV and a maximum magnification of 18.89 KX.

Dry Powder Inhaler Preparation And Their Characterization

The initial step was determining the flow property of gamma oryzanol nanoparticles. Gamma Oryzanol nanoparticles and dehydrated inhalable grade lactose were by hand blended using a geometrical dilution technique at ratios of 1:0.5, 1:1, 1:1.5, etc. to enhance the flow property. At each step of the incorporation of inhalable grade lactose (S1 File), the angles of repose, Carr's index, and Hausner ratio were measured [26]. A dry powder inhaler was optimised based on its exceptional flow characteristics. The optimised formulation was further characterised in terms of zeta size and potential for monitoring DPI changes in nanoparticles. MMAD calculation with a cascade impactor. The aerodynamic diameter below which 50% of the particles remain is known as the mass median aerodynamic diameter, or MMAD. A particle's aerodynamic diameter regulates how much of it deposits in the pulmonary system. An eight step cascade impactor was used to calculate the MMAD of the optimised dry powder inhaler [27]. First, a 28.3 L/min flow rate of DPIs was applied to the cascade impactor. Following the DPI deposition, each chamber's gamma oryzanol concentration was ascertained using (HPLC), in accordance with earlier findings with a few minor modifications [22].

Water as mobile phase: acetonitrile at 70:30 and 1.0 millilitres per minute of flow. At 290 nm, absorbance was found. Each chamber's estimated drug concentration was entered into the {MMAD CALCULATORº to determine the geometric standard deviation (GSD) and MMAD. We determined other metrics, such as the proportion of fine particles and extremely fine particles, based on our previously published studies [28]. The amount released was calculated using drugs found in every step and filter [29]. investigation of in vitro release. After being dissolved in 2 millilitres of simulated lung fluid (SLF) [30], a 5 mg Gamma Oryzanol equivalent dry powder inhaler was put into a dialysis bag. The drug-filled bag was bound over the glass plate and stored at the bottom of the dissolving chamber to prevent it from floating. A 1 litre SLF [28] was used for the in-vitro release research, which was conducted at 37±0.5ÊC and 100 rpm of paddle speed [31]. Fresh SLF was added to 10 ml of dissolving fluid that was removed at predetermined intervals for up to 24 hours. We analysed the in-vitro release data for the zero order models of Highuchi and Korsmeyer-Peppa. Best fitting model was chosen based on correlation coefficient (r2).

Accelerated stability study: A research on accelerated stability was conducted in accordance with ICH guideline Q1A (R2). Cryoprotectant vials covering freshly made dry powder inhalers of Gamma-Oryzanol nanoparticles were sealed with paraffin tap. These vials were maintained at 25±2ÊC and 60±5% RH in a stability chamber. The nanoparticles were examined every six months, once every three months for the first three months and once every six months after that [31–33]. drug entrapment, Zeta size, PDI, zeta potential, and drug release tests were performed to evaluate the constancy of the gamma-oryzanol nanoparticle dry gunpowder inhaler.

3. Results and Discussion

Drug-excipient interaction

The lack of chemical interaction was verified by the FTIR spectra (Figs. 1A and 1B), which also supported the chemical friendliness by preserving the integrity of the principal peaks. The N-H wag peak in a physical combination was discovered at 828.277 cm-1, while it was observed at 823.46 cm-1 in pure gamma-oryzanol. = The C-H bending in the combination and pure Gamma Oryzanol was 899.63 cm-1 and 900.59 cm-1, respectively. Gamma-oryzanol was shown to be compatible with both lactose and chitosan, as evidenced by the N-H stretch, C-C = C stretch , and C = S stretching peak that also appeared at 1591.61 cm-1, 3265.74 cm-1, and 1023.01 cm-1, respectively, with a restricted diffraction range.

Characterization of Chitosan nanoparticles

The gelation process was utilised to create chitosan nanoparticles. The second the Chitosan-gamma-oryzanol solution was added to the TPP solution, cross linking happened. Several iterative optimisations were conducted in order to produce the ideal nanoparticles for the dry powder inhaler. impact of the stirring duration. When the stirring time was increased, the PDE increased first and then reduced while the average particle sizes decreased. Results from dynamic light scattering (DLS) are frequently presented in terms of the z-average, a harmonic mean based on intensity. How small a Gaussian distribution of sizes would be to reflect the fitted DLS data is shown by the polydispersity index, or PDI.

Because of the high PDI, there was a noticeable difference between the z-average value and the average particle size (Table 1). In comparison to the other formulations, Formulation G2 exhibited the greatest PDE of 63.5 ± 0.56%, and its zeta potential value was 30.22 ± 1.88 mV. Values are not statistically significant in the majority of situations. values with a p value that are included in the Table 1. Therefore, the G2 formulation underwent additional alteration.

Table 1: Stirring effect on formulations

Formula Code	Stirring time (minutes)	Zeta potential (mV) **	z-average value (nm) **	Entrapment efficiency (%) **	Average particle size (nm) **	PDI **
G1	15	31.67 ± 2.52	7923 ± 168	52.31 ± 1.85	549.9 ± 52.1	0.994 ± 0.006#
G2	30	30.22 ± 1.88	3236 ± 112	63.5 ± 0.56#	461.9 ± 43.15	0.965 ± 0.029#
G3	45	18.47 ± 3.81	1688 ± 65	46.99 ± 1.8	164.8 ± 36.7	0.992 ± 0.04#
G4	60	26.17 ± 1.97	5544 ± 98	55.69 ± 2.16	243.27 ± 62.08	0.994 ± 0.013#

Values depicted as mean with standard deviation; $^{\#}p$ value less than 0.05

Effect of Chitosan-TPP Ratio

Four fresh batches were made with varying ratios of Chitosan to TPP while maintaining the 30-minute stirring time (G2), and the results were contrasted with the original formulation G2 (Table 2). Based on average particle size, there was no discernible difference between the G2 and GT2, while the GT2's PDI is 0.662 ± 0.005. Because of this, GT2 exhibited a narrower distribution than G2, yielding a z-average value of 1071.67 ± 42.1 nm. Average particle size first dropped, however as TPP quantity grew, this figure climbed once again. Conversely, a rise in the quantity of negative charge TPP resulted in a drop in the Zeta potential value. The average particle size in GT3 was 232.45 ± 24.87 nm; nonetheless, there was a strong association between the PDI value and the z-average value.

Its zeta potential was -9.39 ± 2.13 mV, indicating a greater propensity for solution-based coagulation than GT2. These factors led to additional changes being made to the GT 2 batch. Significant statistical differences were seen between the PDI and certain drug entrapment percentage values.

Table 2: Chitosan:TPP ratio effect

Formula code	z-average value (nm) **	Chitosan: TPP (W/W)	PDI **	Average particle size (nm) **	Drug entrapment (%) **	Zeta potential (mV) **
G2	3424 ± 109	6:1	0.972 ± 0.032$^{\#}$	454.5 ± 31.14	53.5 ± 0.36$^{\#}$	32.21 ± 1.78
GT 2	1071.67 ± 42.1	5:1	0.662 ± 0.005$^{\#}$	472.91 ± 92.21	68.43 ± 1.86	17.61 ± 2.83
GT 3	1634.23 ± 46.52	4:1	0.712 ± 0.005$^{\#}$	232.45 ± 24.87	65.35 ± 2.52	-9.39 ± 2.13
GT 4	5452 ± 115.7	3:1	0.684 ± 0.004$^{\#}$	426.6 ± 27.96	41.37 ± 1.32	1.68 ± 1.02
GT 5	2549.3 ± 143.24	2:1	0.734 ± 0.02$^{\#}$	442.71 ± 32.01	41.15 ± 0.75$^{\#}$	19.44 ± 2.16

Values are mean ± standard deviation, $^{\#}p$ value less than 0.05

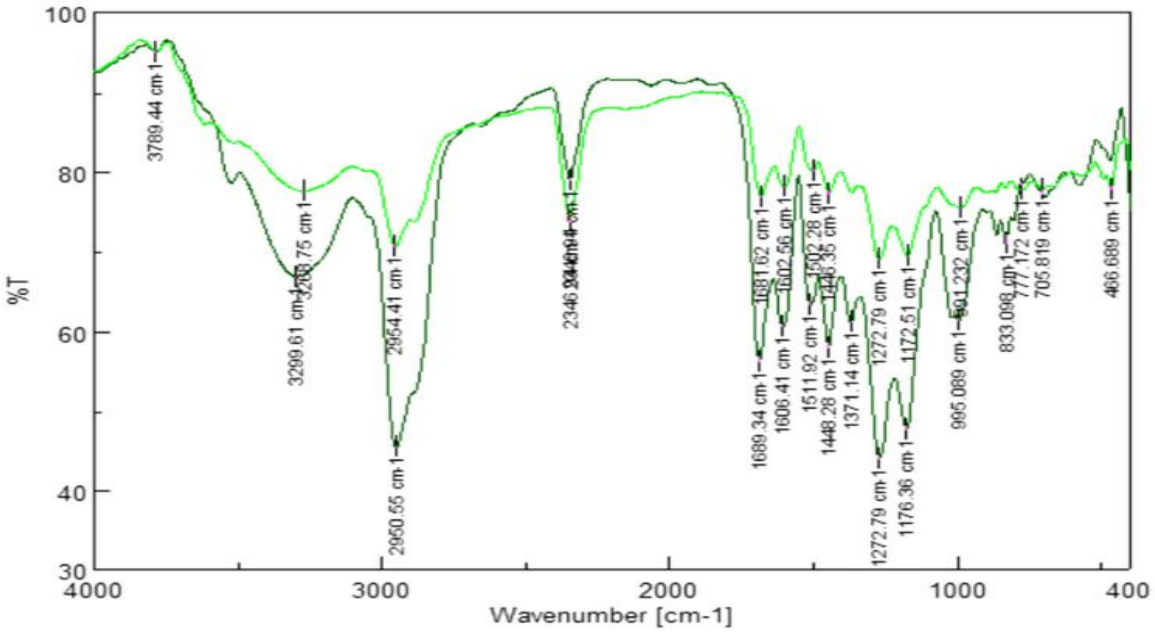

Fig 1: FTIR of gamm oryzanol

Effect of Gamma Oryzanol -Chitosan ratio

In 10 millilitres of 1% acetic acid solution, the amount of chitosan was progressively raised to 90 mg, while the amount of gamma oryzanol remained constant throughout the formulation. An increase in the quantity of Chitosan resulted in a considerable rise in Gamma Oryzanol entrapment. Because of the high PDI in DG6–DG9, no meaningful relationship between the z-average and average particle size was found. For optimisation, average particle size, drug entrapment, and zeta potential were taken into account. DC 6 had the smallest average particle size, yet its PDE was lower than DG 8's after compression. Because of its fewer particles and maximum PDE, DG 8 (which contains 80 mg of

chitin) was chosen as the optimal batch (Table 3). The mean size of the particles and the z-average value did not show a link in any of the cases when the PDI was close to 1.000. As indicated by the p values <0.05 in the Table 3, several of the values were statistically significant. Volume of TPP solution optimisation. The z-average score and PDI showed notable variations when the TPP solution volume was increased to 10 mL (the TPP quantity constant). This marked the last stage in the Gamma Oryzanol nanoparticle optimisation process. In 10mL of water solution, the optimised batch (OP) comprises 50 mg of gamma oryzanol, 80 mg of chitosan, and 16 mg of TPP. A 30-minute stirring period was maintained. The average particle size of 303.77 ± 7.38 nm was substantially associated with the z-average value of 314.37 ± 3.68 nm for the OP batch. The optimised batch's PDE and Zeta potential were determined to be 80.65 ± 0.4% and 32.4 ± 1.04 mV, respectively. It was discovered that the drug entrapment result, PDI, and z-average values of the OP batch were statistically significant. Optimized nanoparticles exhibited reduced propensity to coagulate in both solution and storage.

Table 3: PTH:Chitosan ratio effect

Formula code	PDI **	PTH: Chitosan (mg)	Avg particle size (nm) **	z-average value (nm) **	Drug entrapment (%) **	Zeta potential (mV) **
GT 2	0.654 ± 0.12#	50:50	456.2 ± 79.2	1058.24 ± 25.42	65.68 ± 2.21	14.4 ± 5.4
DG 6	0.989 ± 0.11#	50:60	186.06 ± 25.92	2782.32 ± 38.51	75.9 ± 0.35	34.8± 0.74
DG 7	0.987 ± 0.003#	50:70	254.12 ± 22.5	2872.32 ± 60.12	72.54 ± 0.05	25.6 ± 1.8
DG 8	0.978 ± 0.028#	50:80	235.4 ± 10.57	2946.64 ± 29.81	74.5 ± 0.46#	33.27 ± 1.46
DG 9	0.979 ± 0.002#	50:90	332.5 ± 24.19	2874 ± 57.24	72.72 ± 0.13#	25.6 ± 2.12

Scanning electron microscopy (SEM)

The optimised formulation (OP) nanoparticles were revealed to have a spherical shape by SEM images (Fig 2). The majority of the particles had a size of 301.9 nm, making them appropriate for use in inhalation formulations. In the remaining instances, handling-related moisture entrapment was the cause of aggregation.

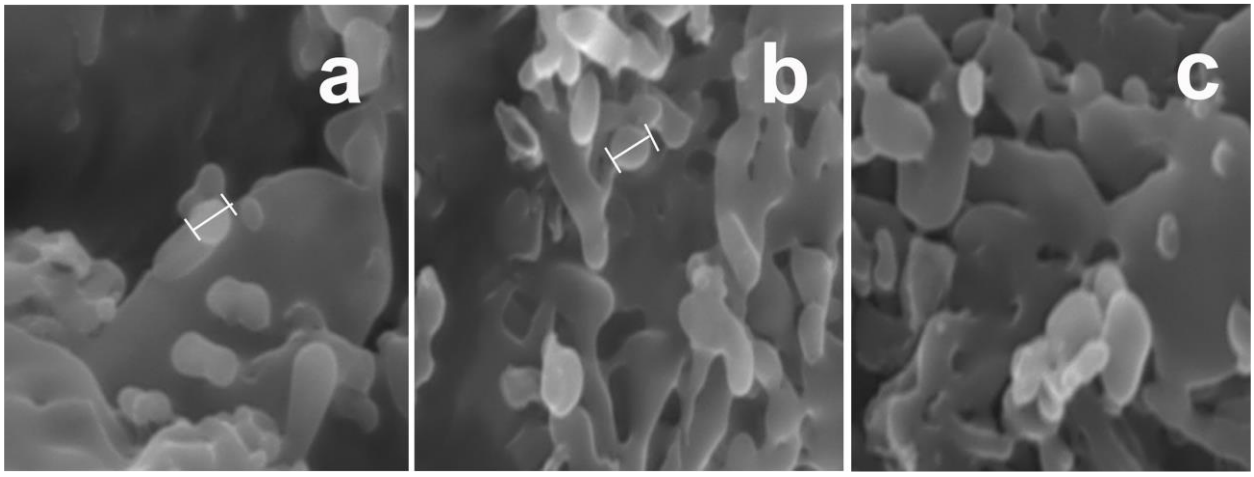

Fig 2: Image of scanning electron microscope of the optimized formulation.

Formulation and Characterization of Dry Powder Inhaler

Deep lung delivery now requires the creation of a sufficient carrier system; nonetheless, selecting one for the pulmonary passage of NPs remains difficult. The carrier should offer the stability of the drug, ease of managing while filling and manufacturing, adequate aerodynamic stability for proper lung accumulation, and improved powder flowability, which helps with drug spread from the inhaler device, in addition to the needed safety about contact with lung tissue [13]. The prepared, freeze-dried nanoparticles had a decent flow performance and were a fluffy mass. The angle of repose, Hausner ratio, and Carr's index for these nanoparticles were 1.21, 17.43%, and 37.32Å, respectively.

Therefore, in order to improve the bulk and flow properties of nanoparticles, specific inhalable type lactose was applied. This specific grade lactose's tiny particles greatly increased the flow properties. Initially, the optimised Gamma-Oryzanol nanoparticles (OP) were mixed physically using a different amount of anhydrous lactose. Hausner ratio, Carr's index, and angle of repose were calculated for each addition of dehydrated lactose . The values obtained for the lactose-gamma oryzanol nanoparticles ratio were 29.25±2.15Ê, 09.76±2.1%, and 1.11±0.01, in that order. After performing zeta analysis on the manufactured DPI having gamma oryzanol nanoparticles, it was determined that there had been no appreciable alterations to the z-average value or zeta potential.

The primary factors that dictate their deposition in the various lung regions are their mass average aerodynamic diameter (MMAD) and particle size. Alveoli and tiny airways can be reached by particles with a size of 0.5±5 μm [40]. DPI deposition was seen at every level of the chamber. The better the dispersion, the higher the carrier concentration [41]. It was discovered that the maximum small particle percentage, extra fine particle fraction, and emitted dosage were, respectively, 81.19%, 18.91%, and 82.37%. Stage 5 showed the highest DPI deposition, which was followed by stages 4 and 6. As a result, the aerodynamic particle size was 1.76 μm with a geometric variance of 1.96. A narrow size distribution centred on a tiny particle size is indicated by a relatively low MMAD and low GSD, which might be advantageous for effective delivery [42]. This indicates that the DPI is ready to reach deep into the lungs.

In-vitro release study

Preparation DPI loaded with nanoparticles of Gamma Oryzanol was tested for drug release behaviour in vitro. The dissolving media utilised to assess the discharge sequence of GO from chitosan nanoparticles was simulated lung fluid with a pH of 7.4 [30]. The prepared Gamma Oryzanol-Chitosan nanoparticles released up to 96.91% in a 24-hour period, with a first explosive release of 22%. The continuous release would enable them to keep the dosage in the lungs for an extended amount of time, while the first burst release would aid in achieving the appropriate plasma concentration in the lungs. comparing the correlation coefficient values of several models, the model that most closely matches the release data is chosen.

A substantial difference was seen at first, but in the latter cases, the majority of the p values were found to be significant. After analysing the in vitro release data using the zero order, Highuchi, and Korsmeyer-Peppa models, the correlation coefficients (r2) were discovered to be, respectively, 0.886, 0.961, and 0.976. The drug release mechanism is described by the release best suited Korsmeyer-Peppa's kinetic model. The fact that the value of ªnº was 0.544 indicates that the release is related to both the erosion and diffusion mechanisms together. Studying stability more quickly. Zeta potential, release profile, drug entrapment, and z-average particle size were used to assess the stability of NPs. Zeta size, zeta potential, PDI, and medication release all showed how the dry powder inhaler was conserved during the stress test. PDE, drug release percentage, zeta potential, PDI, and Zeta potential did not alter significantly. The dissolution of GO from Chitosan nanoparticles was not significantly affected by narrow range changes in particle sizes (Table 4). There was no clustering or aggregation of the particles exhibited in the 6 m accelerated stability test (Fig 2).

Table 4: Accelerated stability study of optimized formulation

Time (month)	Zeta potential	% Drug Entrapment	PDI	z-average (nm)	% drug release in 24 hr
0	27.4 ± 3.5	78.74 ± 0.12	0.412 ± 0.13	322.4 ± 11	95.95 ± 1.5
1.5	27.3 ± 2.5	78.49 ± 0.08	0.428 ± 0.21	327.8 ± 08	97.86 ± 0.9
3	27.3 ± 3.4	78.32 ± 0.13	0.425 ± 0.42	353.4 ± 07	96.71 ± 3.2
6	28.4 ± 2.2	78.14 ± 0.17	0.427 ± 0.37	352.4 ± 14	97.52 ± 3.4

4. Conclusion

Ionic gelation was used to create gamma Oryzanol nanoparticles. The SEM examination verified that the prepared Gamma Oryzanol nanoparticles had a spherical shape and a particle size of 314.37 ± 3.68 nm. Improved Gamma Oryzanol nanoparticles were further developed into a dry powder inhaler with an aerodynamic particle size of 1.76μm, indicating that it was suitable for efficient delivery to the lungs. According to the Korsmeyer-Peppas kinetic model, the in-vitro release investigation indicates that the release happened as a result of a mix of erosion and diffusion mechanisms. The

storage period saw a small variety in particle sizes, however this had no appreciable impact on the release of gamma oryzanol from chitosan nanoparticles. After a single dosage was administered, the prepared DPI kept the concentration of gamma oryzanol above the minimum inhibitory concentration (MIC) for over 12 hours. It can also increase the efficacy of the therapy by raising the concentration of gamma oryzanol in lung tissue at a lower dose.

References

1. Bijev A, Georgieva M. The development of new Tuberculostatics addressing the return of Tuberculosis. J Univ Chem Technol Metall. 2010; 45(2):111±26.
2. Nasiruddin M, Neyaz MK, Das S. Nanotechnology-Based approach in tuberculosis treatment. Tuberc Res Treat [Internet]. 2017; 2017(1):1±12.
3. Lee HW, Kim DW, Park JH, Kim S, Lim M, Phapale PB, et al. Pharmacokinetics of Prothionamide in patients with multidrug-resistant tuberculosis. Int J Tuberc Lungs Dis. 2009; 13(9):1161±6.
4. Lee JK, Cho WH, Bae JW, Kim YU, Bin Park G, Yuk SH, et al. Improvement of Prothionamide dissolution by solid dispersion with complex polymer. Int J Tissue Regen. 2012; 3(1):28±33.
5. Hamilla SM, Michael H, Ashley M. Microparticle drug delivery syringe. In: 2011 IEEE 37th Annual Northeast Bioengineering Conference. 2011. p. 1±2.
6. Debnath SK, Srinivasan S, Debnath M. Development of dry powder inhaler containing Prothionamide-PLGA nanoparticles optimized through statistical design: In-vivo study. Open Nanomed J. 2007; 04:30±40.
7. Deng Q, Zhou C, Luo B. Preparation and characterization of chitosan nanoparticles containing lysozyme. Pharm Biol. 2006; 44(5):336±42.
8. Alsarra IA, Betigeri SS, Zhang H, Evans BA, Neau SH. Molecular weight and degree of deacetylation effects on lipase-loaded chitosan bead characteristics. Biomaterials. 2002; 23:3637±44. PMID:12109689
9. Agnihotri SA, Mallikarjuna NN, Aminabhavi TM. Recent advances on chitosan-based micro- and nanoparticles in drug delivery B. J Control Release. 2004; 100:5±28. https://doi.org/10.1016/j.jconrel.2004. 08.010 PMID: 15491807
10. Patel MP, Patel RR, Patel JK. Chitosan mediated targeted drug delivery system: A review. J Pharm Pharm Sci. 2010; 13(3):536±57.
11. Danaei, M., Dehghankhold, M., Ataei, S., Hasanzadeh Davarani, F., Javanmard, R., Dokhani, A., Khorasani, S., & Mozafari, M. (2018). Impact of particle size and polydispersity index on the clinical applications of lipidic nanocarrier systems. and polydispersity index on the clinical applications of lipidic nanocarrier systems. Pharmaceutics, 10, 57. https://doi.org/10.3390/pharm aceut ics10 020057
12. Donsì, F., Voudouris, P., Veen, S. J., & Velikov, K. P. (2017). Zein-based colloidal particles for encapsulation and delivery of epigallocatechin gallate. Food Hydrocolloids, 63, 508–517. https://doi.org/10.1016/j. foodh yd.2016.09.039
13. Guo, H. X., Heinämäki, J., & Yliruusi, J. (2008). Stable aqueous film coating dispersion of zein. Journal of Colloid and Interface Science, 322(2), 478–484. https://doi.org/10.1016/j.jcis.2007.11.058
14. Huang, M. S., Chanapongpisa, P., Yasurin, P., Kitsubthawee, K., Phetsom J., & Lindayani, I. (2020). Centella asiatica extract loaded BSA nanoparticles using the organic and conventional C. asiatica to improve bioavailability activity and drug delivery system. Applied Science and Engineering Progress, 13(1), 11–18. https://doi.org/10.14416/j.asep.2020.01.001
15. Khalid, N., Kobayashi, I., Neves, M. A., Uemura, K., Nakajima, M., & Nabetani, H. (2017). Encapsulation of β-sitosterol plus γ-oryzanol in O/W emulsions: Formulation characteristics and stability evaluation with microchannel emulsification. Food and Bioproducts Processing, 102, 222–232. https://doi.org/10.1016/j.fbp.2017.01.002
16. Kim, H. W., Kim, J. B., Shanmugavelan, P., Kim, S. N., Cho, Y. S., Kim, H. R., Lee, J. T., Jeon, W. T., & Lee, D. J. (2013). Evaluation of γ-oryzanol content and composition from the grains of pigmented rice-germplasms by LC-DAD-ESI/MS. BMC Research Notes, 6(149), 1–11.
17. Kumar, A., & Dixit, C. K. (2017). Methods for characterization of nanoparticles. In S. Nimesh, C. Ramesh, & N. Gupta (Eds.), Advances in Nanomedicine for the Delivery of Therapeutic Nucleic Acids (pp. 43–58). Woodhead Publishing.
18. Liang, J., Yan, H., Wang, X., Zhou, Y., Gao, X., Puligundla, P., & Wan, X. (2017). Encapsulation of epigallocatechin gallate in zein/chitosan nanoparticles for controlled applications in food systems. Food Chemistry, 231, 19–24. https://doi.org/10.1016/j.foodc hem.2017.02.106
19. Liu, Q., Jing, Y., Han, C., Zhang, H., & Tian, Y. (2019). Encapsulation of curcumin in zein/ caseinate/sodium alginate nanoparticles with improved physicochemical and controlled release properties. Food Hydrocolloids, 93, 432–442. https://doi.org/10.1016/j.foodh yd.2019.02.003
20. Luo, Y., Wang, T. T. Y., Teng, Z., Chen, P., Sun, J., & Wang, Q. (2013). Encapsulation of indole-3-carbinol and 3,3′-diindolylmethane in zein/carboxymethyl chitosan nanoparticles with controlled release property and improved stability. Food Chemistry, 139(14), 224–230. https://doi.org/10.1016/j.foodc hem.2013.01.113
21. Rajan M, Raj V. Encapsulation, characterisation and in-vitro release of anti-tuberculosis drug using Chitosan- oly Ethylene Glycol nanoparticles. Int J Pharm Pharm Sci. 2012; 4(4):255±9.

22. Luo Y, Zhang B, Cheng W, Wang Q. Preparation, characterization and evaluation of selenite-loaded chitosan / TPP nanoparticles with or without zein coating. Carbohydr Polym. 2010; 82(3):942±51.
23. Dadras OG, Sadeghi MA, Mohammad Farhangi N. Preparation, characterization and in vitro studies of chitosan nanoparticles containing Androctonus Crassicauda scorpion venom. J Appl Chem Res. 2013; 7(3):35±46.
24. Othayoth R, Karthik V, Kumar SK. Development and characterization of chitosan pluronic nanoparticles for Tamoxifen delivery and cytotoxicity to MCF -7 cells. In: International Conference on Advanced Nanomaterials & Emerging Engineering Technologie. 2013. p. 394±401.
25. Rezaei MA, Alonso MJ. Preparation and evaluation of chitosan nanoparticles containing Diphtheria toxoid as new carriers for nasal vaccine delivery in mice. Arch Razi Inst. 2006; 61(1):13±25.
26. Pilicheva B, Katsarov P, Kassarova M. Flowability evaluation of dry powder inhalation formulations intended for nasal delivery of Betahistine Dihydrochloride. Sikk Manipal Univ Med J. 2014; 2(1):77±90.
27. Sinha B, Mukherjee B. Development of an inhalation chamber and a dry powder inhaler device for administration of pulmonary medication in animal model. Drug Dev Ind Pharm. 2012; 38(2):171±9. https://doi.org/10.3109/03639045.2011.592532 PMID: 21721851
28. Debnath SK, Saisivam S, Omri A. PLGA Ethionamide nanoparticles for pulmonary delivery: Development and in vivo evaluation of dry powder inhaler. J Pharm BiAvailable from: http://dx.doi.org/10.1016/j.jpba.2017.07.051
29. Pascal D, Paul H, Anne DBH, Henderik FW. The clinical relevance of dry powder inhaler performance for drug delivery. Respir Med [Internet]. 2014; 108(8):1195±203. https://doi.org/10.1016/j.rmed.2014.05.009 PMID: 24929253
30. Marques MRC, Loebenberg R, Almukainzi M. Simulated biological fluids with possible application in dissolution testing. Dissolution Technol. 2011; 18(3):15±28.
31. 31. May S, Jensen B, Wolkenhauer M, Schneider M, Lehr CM. Dissolution techniques for in vitro testing of dry powders for inhalation. Pharm Res. 2012; 29(8):2157±66. https://doi.org/10.1007/s11095-012-0744-2 PMID: 22528980
32. Hao J, Fang X, Zhou Y, Wang J, Guo F, Li F, et al. Development and optimization of solid lipid nanoparticle formulation for ophthalmic delivery of chloramphenicol using a Box-Behnken design. Int J Nanomedicine. 2011; 6:683±92. https://doi.org/10.2147/IJN.S17386 PMID: 21556343
33. ICH Expert Working Group. ICH Guideline Q1A(R2) Stability Testing of New Drug Substances and Products. In: International Conference on Harmonization. 2003. p. 24.
34. Fernandes CA, Vanbever R. Preclinical models for pulmonary drug delivery. Expert Opin Drug Deliv . 2009; 6(11):1231±45. https://doi.org/10.1517/17425240903241788 PMID: 19852680 NCI. Equivalent surface area dosage conversion factors [Internet]. Vol. 50, The Frederick National Lab Animal Care and Use Committee. 2012. p. 1±2.